Transient Convection, Diffusion, and Adsorption in Surface-Based Biosensors

Rasmus Hansen,*,[†] Henrik Bruus,[‡] Thomas H. Callisen,[§] and Ole Hassager*,[†]

[†]Department of Chemical and Biochemical Engineering, Technical University of Denmark, DTU Chemical Engineering Building 227, DK-2800 Kongens Lyngby, Denmark

[‡]Department of Micro- and Nanotechnology, Technical University of Denmark, DTU Nanotech Building 345 B, DK-2800 Kongens Lyngby, Denmark

[§]Novozymes A/S, Novo Allé, 2880 - Bagsværd, Denmark

ABSTRACT: This paper presents a theoretical and computational investigation of convection, diffusion, and adsorption in surface-based biosensors. In particular, we study the transport dynamics in a model geometry of a surface plasmon resonance (SPR) sensor. The work, however, is equally relevant for other microfluidic surface-based biosensors, operating under flow conditions. A widely adopted approximate quasi-steady theory to capture convective and diffusive mass transport is reviewed, and an analytical solution is presented. An

expression of the Damköhler number is derived in terms of the nondimensional adsorption coefficient (Biot number), the nondimensional flow rate (Péclet number), and the model geometry. Transient dynamics is investigated, and we quantify the error of using the quasi-steady-state assumption for experimental data fitting in both kinetically limited and convection-diffusion-limited regimes for irreversible adsorption, in specific. The results clarify the conditions under which the quasi-steady theory is reliable or not. In extension to the well-known fact that the range of validity is altered under convection-diffusion-limited conditions, we show how also the ratio of the inlet concentration to the maximum surface capacity is critical for reliable use of the quasi-steady theory. Finally, our results provide users of surface-based biosensors with a tool for correcting experimentally obtained adsorption rate constants.
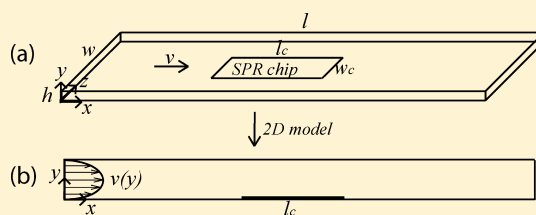
INTRODUCTION

This work investigates transient convection, diffusion, and adsorption in surface-based biosensors. Even though surface plasmon resonance (SPR) sensors have formed the principal basis for this investigation, it is of equal relevance to other related methods, where a sensor surface is placed in a flow cell unit, which is continuously perfused with sample. Such biosensors are used in diverse areas, such as for DNA hybridization,[1,2] chemiluminescence detection,[3] and cell attachment and release from surfaces.[4] From a theoretical viewpoint, similar physics also occur in other systems, such as protein microarrays.[5] Theoretical research, related to biosensor applications, typically attempts to include novel mechanisms, such as the ac electrothermal (ACET) effect,[6] or aims at developing analytical and semianalytical models for better data interpretation.[7,8]

Surface plasmon resonance (SPR) spectroscopy, in particular, is an advanced optical sensing method that enables label free monitoring of macromolecular interactions. The technique is widely used in biomolecular research, medical diagnostics, food analysis, and environmental monitoring.[9,10] In particular, SPR sensors are used to study macromolecular interactions at the surface of a sensor chip, where so-called ligand molecules have been immobilized. The overall principle of SPR is that adsorption of analyte to the sensor chip surface changes the

refractive index of the surface, which is detected by an optical reader.[11]

While the SPR technique, developed and commercialized by, for example, Biacore, is well capable of capturing qualitative behavior, quantitative studies of chemical rate constants and equilibrium constants are more challenging. Inconsistencies in derived rate constants have led to both experimental and theoretical investigations of the effect of convection and diffusion on the SPR signal.[12,13] Significant progress was made by the application of a quasi-steady-state approximation, that is, a steady-state bulk mass transport coupled to a dynamic adsorption scheme (explained in detail below). This approximation has been widely adopted for Biacore data analysis.[13−19] However, practice in the biochemical society still, to a large degree, consists of empirical and qualitative studies.[20−23]

The quasi-steady-state approximation leads to a nondimensional number called the Damköhler number, which is sometimes referred to as the limit coefficient. An expression of the Damköhler number is derived in terms of the nondimensional adsorption coefficient (Biot number), the nondimensional flow rate (Péclet number), and the model geometry. The ability of the quasi-steady theory to capture

mass transport is thoroughly tested, by comparison with numerical simulations of the transient dynamics. In this way, the consequences of using the quasi-steady theory for experimental data fitting in both kinetically limited and convection-diffusion limited regimes are properly quantified.

■ THEORY

This section provides a theoretical treatment of mass transport, that is, convection, diffusion, and adsorption, in a microfluidic device with a surface-based biosensor. We consider only unimolecular systems, that is, a single solute in solution. First, the system geometry is presented, along with the evolution equations governing the system dynamics. We present results of using two different time scales, namely, a kinetic time and a diffusion time, with the former proving useful if adsorption kinetics is slow compared to bulk mass transport to the surface, and the latter proving useful in the opposite case. The nondimensional parameters are discussed, and estimates of numerical values are provided. The section ends with a thorough description and analysis of the quasi-steady theory, including a discussion of its inherent parameter: the Damköhler number. The analysis contains an analytical solution of the quasi-steady theory.

System Geometry and 2D Approximation. We investigate transport dynamics in a model geometry of a surface plasmon resonance (SPR) sensor, which by far is the most common SPR platform used.[24] The finite distance from the inlet of the microfluidic
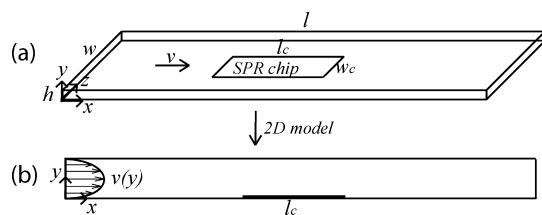
Figure 1. (a) Rectangular flow cell of length l, height h, and width w. The SPR chip of length l_c and width w_c is indicated as the square in the middle of the flow cell. The buffer flow is represented by the velocity vector v. (b) Two-dimensional approximation of the system in the vertical xy-plane. The parabolic velocity profile is indicated at the inlet of the flow cell.

flow cell to the sensor surface is included, as shown in Figure 1. The length scales are l = 2.3 mm, w = 0.5 mm, and h = 0.02 mm. Adsorption is probed by the SPR chip located on the surface in the middle of the flow cell. The SPR chip has a length of l_c = 0.6 mm and a width of w_c = 0.16 mm. The fluid flows in the lengthwise direction (x), with a parabolic velocity profile along the direction (y) of the height of the flow cell, that is, $v_x(y) = 4v_m(y/h)(1 - y/h)$, where v_m is the maximum velocity. Based on the large geometric aspect ratio $w/h = 10$ and the small Reynolds numbers often present in the system, we have assumed total invariance in the direction (z) of the width of the flow cell,[25] essentially ending up with a two-dimensional consideration of the transport. Hereby we do not take boundary effects from the side walls of the flow cell at $z = \{0,w\}$ into account.

Evolution Equations. We define two dependent variables, namely, the bulk concentration field $c = c(x,y,t)$ and the surface concentration field $\gamma = \gamma(x,t)$, where t is time. We name the bulk domain Ω, nonadsorbing surface domains $\partial\Omega$, and surfaces where adsorption takes place $\partial\Omega_{ads}$. The spatiotemporal evolution of the bulk concentration field $c = c(x,y,t)$ is governed by the convection-diffusion equation

$$\frac{\partial c}{\partial t} + v_x(y)\frac{\partial c}{\partial x} = D\nabla^2 c, \quad (x, y) \in \Omega \quad (1)$$

where the Laplacian $\nabla^2 = \partial^2/\partial x^2 + \partial^2/\partial y^2$ and D is the diffusion coefficient. The boundary conditions for the bulk concentration are given by

$$\frac{\partial c}{\partial y} = 0, \quad y \in \partial\Omega \quad (2)$$

$$-D\frac{\partial c}{\partial y} = -\mathcal{A}(\gamma, c), \quad y \in \partial\Omega_{ads} \quad (3)$$

The former is simply a no-flux condition, whereas the latter is a balance between diffusive flux perpendicular to the surface and net adsorption rate, captured in the adsorption term $\mathcal{A}(\gamma,c)$ in eq 5. At the inlet of the flow cell, at $x = 0$, the concentration is equal to the injection concentration, $c = c_0$. At the outlet of the flow cell, $x = l$, we assume free convection, that is, essentially $\partial c/\partial x = 0$. The spatiotemporal evolution of the surface concentration field $\gamma = \gamma(x,t)$ is governed by the adsorption-diffusion equation[26]

$$\frac{\partial\gamma}{\partial t} - \frac{\partial}{\partial x}\left[D_s\frac{\partial\gamma}{\partial x}\right] = \mathcal{A}(\gamma, c), \quad \partial\Omega_{ads} \quad (4)$$

where D_s is the surface diffusion coefficient, which in general can be a function of both the independent variables, x and t, as well as the dependent variables γ and c. The adsorption term $\mathcal{A}(\gamma,c)$ represents the net rate of change of surface concentration due to adsorption and desorption, and is determined by the kinetics of some chosen adsorption−desorption scheme. $\mathcal{A}(\gamma,c)$ can, in general, include arbitrarily complex surface kinetics. No-flux boundary conditions for γ, that is, $\partial\gamma/\partial x = 0$, are imposed at the end of the adsorbing domain; that is, surface bound molecules only leave the chip by desorption.

Adsorption Kinetics. The adsorption kinetics is modeled by a phenomenological model, which ultimately captures experimental data and thereby provides reasonable and consistent phenomenological parameters. The standard adsorption model that still contains the feature of a maximum surface capacity γ_m is the Langmuir adsorption model. This model is essentially a first order scheme between bulk molecules at the interface $c|_{y=0}$ and free surface sites ($\gamma_m - \gamma$), with adsorption rate constant k_a and desorption rate constant k_d. This first order model may be written in the form

$$\mathcal{A}(\gamma, c) = k_a c|_{y=0}(\gamma_m - \gamma) - k_d\gamma \quad (5)$$

When $c|_{y=0}$ is independent of γ, this is a linear relation between $\mathcal{A}(\gamma,c)$ and γ. This particular adsorption model is a *local theory* in both space and time; that is, the evolution of γ at (x,t) depends only on the present state at (x,t). The ultimate goal is often to obtain consistent values for the triplet (k_a,k_d,γ_m) of phenomenological parameters from experimental biosensor data. In this linear model, the adsorption and desorption rate constants, k_a and k_d, respectively, are assumed unaltered by the density on the surface. In reality, one might expect interactions between adsorbed particles at high densities. However, in spite of its simplicity, it has been argued that this model is general enough to explain the majority of adsorption/desorption processes in molecular biology.[8] Substituting eq 5 into eq 4 and eq 3, these two equations together with eq 1, and the remaining boundary conditions, form a nonlinear system of partial differential equations for the two concentration fields $c = c(x,y,t)$ and $\gamma = \gamma(x,t)$. The system is of such complexity that a numerical study is necessary for detailed analysis.

Nondimensional Parametrization. Nondimensional formulations are developed for a more comprehensible parametrization of the evolution equations. Two different nondimensional formulations are introduced and discussed.

Nondimensional Parametrization: Kinetic Scaling. In order to put the evolution equations on nondimensional form, we introduce the following spatial and temporal scales:

$$\bar{x} = \frac{x}{h}, \quad \bar{y} = \frac{y}{h}, \quad \bar{t} = k_a c_0 t \quad (6)$$

Note in particular that time has been made nondimensional by the adsorption rate. For the dependent concentration variables, we introduce the following scaled dependent variables:

$$\bar{c} = \frac{c}{c_0}, \quad \bar{\gamma} = \frac{\gamma}{\gamma_m} \quad (7)$$

In terms of these nondimensional variables and the definitions $f(\bar{y}) = 4\bar{y}(1 - \bar{y})$, $\bar{\nabla}^2 = \partial^2/\partial\bar{x}^2 + \partial^2/\partial\bar{y}^2$, we obtain the nondimensional evolution equation for the bulk concentration field

$$\text{Bi}\bar{c}_0\frac{\partial\bar{c}}{\partial\bar{t}} + \text{Pe}f(\bar{y})\left(\frac{\partial\bar{c}}{\partial\bar{x}}\right) = \bar{\nabla}^2\bar{c}, \quad \Omega \tag{8}$$

with the boundary condition (eq 3) given by

$$\left.\frac{\partial\bar{c}}{\partial\bar{y}}\right|_{\bar{y}=0} = \text{Bi}\bar{c}|_{\bar{y}=0}(1 - \bar{\gamma}) - K\text{Bi}\gamma, \quad \partial\Omega_{\text{ads}} \tag{9}$$

The nondimensional evolution equation for the surface concentration field is given by

$$\frac{\partial\bar{\gamma}}{\partial\bar{t}} - \frac{\partial}{\partial\bar{x}}\frac{d_s}{\text{Bi}\bar{c}_0}\frac{\partial\bar{\gamma}}{\partial\bar{x}} = \bar{c}|_{\bar{y}=0}(1 - \bar{\gamma}) - K\gamma, \quad \partial\Omega_{\text{ads}} \tag{10}$$

The remaining boundary conditions are trivially translated into the nondimensional form. These nondimensional evolution equations are parametrized by the following five nondimensional groups.

$$\text{Pe} = v_m h/D \tag{11}$$

$$\text{Bi} = k_a\gamma_m h/D \tag{12}$$

$$\bar{c}_0 = c_0 h/\gamma_m \tag{13}$$

$$K = k_d/k_a c_0 \tag{14}$$

$$d_s = D_s/D \tag{15}$$

The Péclet number Pe measures the ratio of transport by convection to perpendicular diffusion and is essentially the nondimensional flow rate. The Biot number Bi measures the ratio of adsorption rate to diffusion along the height of the flow cell and is essentially the nondimensional adsorption rate constant. $\bar{c}_0$ is a nondimensional inlet concentration. In the limit of no flow, $\bar{c}_0$ is the reciprocal of the fraction of the height h needed to fill the surface up to $\gamma = \gamma_m$. This interpretation explains the close relationship between $\bar{c}_0$ and the so-called depletion depth introduced by ref 27. K is the kinetic equilibrium constant. d_s is the ratio of the surface and bulk diffusion coefficients, and if $D_s < D$, $d_s \in \{0,1\}$ measures the hindrance of diffusion caused by the presence of the surface. Interestingly, the magnitude of the transient term in eq 8 is weighed by the product $\bar{c}_0\text{Bi} = k_a c_0 h^2/D$, meaning essentially that adsorption dynamics for large inlet concentrations of molecules with a high affinity to the surface evolves in a transient regime. This result is supported by Squires et al.[28] in their eq 21.

Nondimensional Parametrization: Diffusion Scaling. Following a similar approach as above, but with the difference of scaling time with a diffusion time, that is, $\bar{t} = Dt/h^2$, the nondimensional evolution equation for the bulk concentration field takes the form

$$\frac{\partial\bar{c}}{\partial\bar{t}} + \text{Pe}f(\bar{y})\left(\frac{\partial\bar{c}}{\partial\bar{x}}\right) = \bar{\nabla}^2\bar{c}, \quad \Omega \tag{16}$$

while the boundary condition (eq 3) is now given by

$$\left.\frac{\partial\bar{c}}{\partial\bar{y}}\right|_{\bar{y}=0} = \text{Bi}\bar{c}|_{\bar{y}=0}(1 - \bar{\gamma}) - K\text{Bi}\bar{\gamma}, \quad \partial\Omega_{\text{ads}} \tag{17}$$

The nondimensional evolution equation for the surface concentration field becomes

$$\frac{\partial\bar{\gamma}}{\partial\bar{t}} - \frac{\partial}{\partial\bar{x}}d_s\frac{\partial\bar{\gamma}}{\partial\bar{x}} = \text{Bi}\bar{c}_0\bar{c}|_{\bar{y}=0}(1 - \bar{\gamma}) - K\text{Bi}\bar{c}_0\bar{\gamma}, \quad \partial\Omega_{\text{ads}} \tag{18}$$

The correspondence between the time scales for kinetic scaling (ks) and diffusion scaling (ds) are

$$\bar{t}^{\text{ks}} = \bar{t}^{\text{ds}}k_a c_0 h^2/D = \text{Bi}\bar{c}_0\bar{t}^{\text{ds}} \tag{19}$$

Kinetic/Diffusion Limitation and the Role of Scaling. The kinetic scaling of time is particularly advantageous in the regime of kinetically limited dynamics. Generally speaking, kinetically limited dynamics is characterized by a stronger dependence on the adsorption kinetics (Biot number) than on the convection and diffusion (Péclet number). On the other hand, if the adsorbing molecules have a very high affinity to the surface, the Biot number Bi ≫ 1. In this limit, the dynamics is convection-diffusion limited, which is characterized by a stronger dependence on convection and diffusion than on the adsorption kinetics. In this limit, it is advantageous to use the diffusion scaling of time. Disregarding the dynamical limit of the system, there are other pros and cons for applying the two different time scales. As seen below, the quasi-steady theory adopts a minimal number of nondimensional parameters by using kinetic scaling. Hence, kinetic scaling is advantageous when working with the quasi-steady theory. This is consistent with the fact that the quasi-steady-state approximation is only theoretically supported for kinetically limited dynamics. This is further elaborated on in the later section on the quasi-steady theory. Usually, k_a is a parameter one wishes to determine from an adsorption experiment. It is therefore unknown a priori, whereby kinetic scaling is not practical for experimental data fitting. This issue is avoided by using diffusion scaling. Dependent on the experimental regime, it might as well be preferable to present and fit experimental data unscaled.

Estimates of Nondimensional Numbers. In this section, we estimate some reasonable values for the nondimensional numbers. Concerning typical operating conditions, flow rates are in the range $Q = 1-100 \ \mu\text{L min}^{-1}$, which amounts to maximum velocities of $v_m = 3Q/2hw = 10^{-3}-10^{-1} \ \text{ms}^{-1}$. Injection concentrations typically range from $c_0 = 10^{-1}-10^2 \ \mu\text{M}$. To proceed, we need to consider a model binder. We take as an example[30] a globular protein with a diameter of $2R = 5$ nm and molecular weight $M_w = 30 \ \text{kDa} = 3 \times 10^4 \ \text{g mol}^{-1}$. A simple estimate of the maximum surface capacity γ_m is simply the weight of one molecule divided by its diameter squared. Namely, $\gamma_m = M_w/4N_A R^2 \approx 2 \times 10^3 \mu\text{g m}^{-2}$, where N_A is the Avogadro number. However, in biochemical, studies the surface of the chip, or the dextran layer, is sometimes prepared with a relatively low number of binding sites, with the aim of reducing rebinding probability and neighbor interactions among the adsorbing binders. This implies that the above estimate for γ_m, which is based on a packing occurring for, for example, self-assembled monolayers, represents an upper limit. In several applications, the maximum surface capacity can be significantly lower. The diffusion coefficient can be estimated from the Stokes−Einstein relation. In aqueous solution at room temperature, the dynamic viscosity is $\mu \approx 10^{-3} \ \text{N s m}^{-2}$, and $T \approx 300 \ \text{K}$, hence $D = k_B T/6\pi\mu R \approx 10^{-10} \ \text{m}^2 \ \text{s}^{-1}$.

Based on the above values, we can estimate the regime of the nondimensional numbers. By choosing $c_0 \approx 1 \ \mu\text{M}$, we obtain $\bar{c}_0 = c_0 h/\gamma_m \approx 1$, in the case of close packing on the surface. For surfaces prepared with a lower number of binding sites, $\bar{c}_0 > 1$. For the Péclet number, we obtain $\text{Pe} = v_m h/D \approx 5 \times 10^2-5 \times 10^4$.

The Quasi-Steady Theory. Ideally, one would like to interpret SPR data by assuming simply that the concentration near the sensor $c_{y=0}$ is identical to the injection concentration c_0, that is by assuming that there is no resistance to mass transfer. To account for the corrections due to some mass transfer resistance, it has been suggested to interpret data by means of a mass transport model, saying that the overall flux of solute J to the surface is proportional to the difference between the far field concentration c_0, usually taken as the injection concentration, and the concentration close to the surface of the sensor $c|_{y=0}$, that is, $J = k_L(c_0 - c|_{y=0})$. In fact, this is based on a solution to the stationary diffusion-convection equation for the concentration field $c = c(x,y)$ on a semi-infinite domain $x,y \geq 0$.

$$v_x\frac{\partial c}{\partial x} = D\frac{\partial^2 c}{\partial y^2}, \quad y > 0 \tag{20}$$

The velocity $v_x = v_x(y)$ is linearized close to the surface, that is, $v_x(y) = \dot{\gamma}_w y$, with $\dot{\gamma}_w$ being the shear rate at the surface, and the boundary conditions for the concentration field are $c(x,y)|_{y=0} = \text{const}$, $c(x,y)|_{x,y\to\infty}$

= 0, and $c(x,y)|_{x=0} = c_0$. The solution consists of a concentration boundary layer close to the surface $y = 0$, and a flux of solute to the surface $J = k_L(c_0 - c|_{y=0})$, where the mass transport parameter k_L is given by[26]

$$k_L = \frac{2D}{\Gamma\left(\frac{7}{3}\right)}\left(\frac{\dot{\gamma}_w}{9Dl}\right)^{1/3} \tag{21}$$

This mass transport parameter is often chosen as a free fitting parameter, although it may in fact be predicted from the operating conditions. Given a flow rate Q, the shear rate at the wall is

$$\dot{\gamma}_w = \frac{6Q}{h^2 w} \tag{22}$$

The coupling of this stationary convection-diffusion solution with the adsorption kinetics on the surface is performed by loosening up the Dirichlet boundary condition $c(x,y)|_{y=0} = \text{const}$. Letting these bulk particles $c|_{y=0}$ adsorb, they are converted into surface particles γ, and a simple mass balance on the surface dictates $J = d\gamma/dt = \mathcal{A}(\gamma,c)$. The critical assumption here is that the adsorption is so slow that the bulk concentration on the surface $c|_{y=0}$ is practically constant, and use of the steady-state flux $J = k_L(c_0 - c|_{y=0})$, with k_L given by eq 21, is still reasonable.

Inserting the steady-state flux into the mass balance on the surface, we obtain $k_L(c_0 - c|_{y=0}) = \mathcal{A}(\gamma,c)$. In the case of linear kinetics (eq 5), this becomes an algebraic equation for $c|_{y=0}$, with the solution

$$c|_{y=0} = \frac{k_L c_0 + k_d \gamma}{k_a(\gamma_m - \gamma) + k_L} \tag{23}$$

Substituting this into eq 5 gives the following nonlinear ordinary differential equation for the evolution of the surface concentration $\gamma = \gamma(t)$

$$\frac{d\gamma}{dt} = \frac{k_a k_L c_0(\gamma_m - \gamma) - k_d k_L \gamma}{k_a(\gamma_m - \gamma) + k_L} \tag{24}$$

Using kinetic scaling, we can write eq 24 as

$$\frac{d\bar{\gamma}}{d\bar{t}}^{ks} = \frac{1 - (1 + K)\bar{\gamma}}{1 + Da(1 - \bar{\gamma})} \tag{25}$$

with the additional introduction of the important nondimensional Damköhler number

$$Da = k_a \gamma_m / k_L \tag{26}$$

which is the ratio of the adsorption rate and the rate of mass transport to the surface. The Damköhler number measures the limiting effect of convection-diffusion on the adsorption process. In terms of the Damköhler number, the basic assumption of slow adsorption translates to $Da \ll 1$. For increasing Damköhler numbers, the theory is not expected to correctly capture the adsorption dynamics. In a later section, we quantify the deviation from full numerical treatments for increasing Damköhler numbers. Note that when $Da = 0$, we recover

$$\frac{d\bar{\gamma}}{d\bar{t}}^{ks} = 1 - (1 + K)\bar{\gamma}, \quad Da = 0 \tag{27}$$

which is simply the nondimensional form of eq 5, that is, a purely adsorption-limited, linear, kinetic process. Also, the initial rate of adsorption, starting from the initial condition of zero surface concentration, $\bar{\gamma} = 0$, is predicted to be

$$\frac{d\bar{\gamma}}{d\bar{t}}(0)^{ks} = \frac{1}{1 + Da} \quad \text{or} \quad \frac{d\gamma}{dt}(0)^{ks} = c_0 k_L \frac{Da}{1 + Da} \tag{28}$$

Using diffusion scaling, the formulation of the quasi-steady theory involves the two additional parameters, Bi and $\bar{c}_0$, namely,

$$\frac{d\bar{\gamma}}{d\bar{t}}^{ds} = \frac{Bi\bar{c}_0(1 - \bar{\gamma}) - K\bar{\gamma}}{Da(1 - \bar{\gamma}) - 1} \tag{29}$$

Correspondence between the Damköhler, Biot, and Péclet Number. The kinetic scaling of the evolution equations (eqs 8−10) clarifies the assumptions in the quasi-steady theory. By setting Bi = 0, we essentially obtain the conditions for the solution in eq 21; that is, time dependency drops out of the bulk convection-diffusion equation, consistent with an instantaneous buildup of the concentration boundary layer above the adsorbing surface in the *quasi-steady* theory. In addition, the quasi-steady theory approximates reality by a semi-infinite bulk domain, a linear velocity profile, and no inlet distance to the sensor surface. The latter assumption implies a constant concentration field along the *y*-axis at the *x*-value where the sensor surface begins.

The kinetically scaled quasi-steady theory in eq 25 is parametrized only by the Damköhler number Da and the equilibrium constant K. As the quasi-steady theory combines steady-state convection-diffusion with adsorption in the Damköhler number, through the mass transport coefficient k_L, it is naturally possible to express the Damköhler number in terms of the Péclet number and the Biot number. First, from eq 22, $\dot{\gamma}_w = 4v_m/h$. By defining the number $\alpha = 2(4/9)^{1/3}/\Gamma(7/3) \approx 1.2819$, the mass transport coefficient k_L can be expressed as

$$k_L = \alpha\left(\frac{v_m h}{D}\right)^{1/3}\frac{D}{l^{1/3}h^{2/3}}$$

Hence, the Damköhler number is given by

$$Da = \frac{k_a \gamma_m}{k_L} = \alpha^{-1}(l/h)^{1/3}BiPe^{-1/3} \tag{30}$$

Note that the quasi-steady theory is parametrized by the Damköhler number and at the same time is based on the assumption Da = 0. It is clear from eq 30 that the Damköhler number increases linearly with the Biot number and decreases with the cubic root of the Péclet number. Practically speaking, if the binders adsorb fast to the surface (large Biot number), it may be impossible to reduce the Damköhler number significantly by simply increasing the flow rate, that is, Péclet number.

Analytical Solution of the Quasi-Steady Theory. Equation 25 can be solved analytically in *implicit* form, that is, $\bar{t} = \bar{t}(\bar{\gamma})$ instead of the *explicit* form $\bar{\gamma} = \bar{\gamma}(\bar{t})$. It is determined simply by separation of variables and integration, with initially $\bar{\gamma}(\bar{t} = 0) = 0$:

$$\bar{t} = \frac{Da\kappa\bar{\gamma} - (\kappa + Da(\kappa - 1))\ln(1 - \kappa\bar{\gamma})}{\kappa^2} \tag{31}$$

where $\kappa \equiv 1 + K$. For irreversible adsorption $K = 0$, $\kappa = 1$, the solution condenses into

$$\bar{t} = Da\bar{\gamma} - \ln(1 - \bar{\gamma}) \tag{32}$$

This solution may not be so useful for physical insight, but has its practical advantage when performing nonlinear least-squares data fitting in the time domain. Data fitting in the time domain involves a numerical solution of the ordinary differential equation (eq 25) at every parameter space iteration, which can be avoided with the *implicit* solution above. Another option is simply fitting data in the phase plane.[29] This method also does not involve the solution of eq 25, is *explicit*, but as a trade-off involves differentiation of data.

■ NUMERICAL RESULTS AND DISCUSSIONS

This section is concerned with numerical simulations of the dynamics of real adsorption experiments in surface-based biosensors, as described by eqs 8−10, or similarly eqs 16−18. (Collectively referred to as the *simulations*.) In particular, we investigate the quality of the quasi-steady theory by comparison with the numerical simulations. Deviations between the simulations and the quasi-steady theory reveal the effects of the transient dynamics in the simulations, which of course are also present in real adsorption experiments. The results are presented and analyzed in the phase plane, spanned by the mean surface concentration $\Gamma \equiv (1/l_c)\int_{\text{sensor}}\bar{\gamma}\,dx$ and its time

derivative $\dot{\Gamma} \equiv (1/l_c) \int_{sensor} \partial\gamma/\partial\bar{t}\, dx$. This representation clearly illustrates the transient regime, and is the most straightforward approach to analyze deviations from linear adsorption kinetics due to mass transport. A typical procedure for interpreting data from adsorption experiments is to fit the data with the quasi-steady theory eq 24 to reveal an adsorption rate constant k_a.[20−23] To mimic this procedure, we fit the quasi-steady theory, using a least-squares method, to the simulation with Bi as the free fitting parameter. Since the quasi-steady theory has no chance of fitting initial data, the simulation time from the origin of the phase plane to the extremum (highest adsorption rate) is cut off in the fitting procedure, corresponding to typical practice of representing SPR data in the phase plane, that is, Goren et al.[29] The error of the quasi-steady theory is then quantified by the relative difference between the fitted Bi number and the real Bi number used for the simulation. Strictly speaking, we define the error as $(\mathrm{Bi}^{fit} - \mathrm{Bi})/\mathrm{Bi}$. The choice of parameters spans both kinetically limited and convection-diffusion limited dynamics; hence, the results are presented using both kinetic and diffusion scaling of time. Note in particular that purely kinetically limited dynamics, that is, the linear kinetics in eq 5, is represented by a linear curve in the phase plane. The universality characteristic of kinetic scaling is that this linear curve is the diagonal from the point $(0,1)$ on the ordinate to the point $(1,0)$ on the abscissa. We take offset in the estimated regime for the nondimensional parameters and, to constrain the available parameter space, choose to consider the case of irreversible adsorption of binders, which are immobile on the surface, hence $K = d_s = 0$.

Kinetic Scaling. Figure 2 contains a representative collection of phase plane curves using kinetic scaling, that is,

scales linearly with $\bar{c}_0$, taken into account in the kinetic scaling of time in eq 25. Hence the quasi-steady theory does not explicitly include the $\bar{c}_0$ degree of freedom, whereby essentially only two distinctive predictions occur in Figure 2. In this way, the thin black curves denoted (QST) are identical in Figure 2a and b, as well as in Figure 2c and d. Several points are immediately apparent from the simulations. The simulation curves start at the origin of the phase plane, whereas the quasi-steady theory has the finite initial adsorption rate given in eq 28. It is important to note that the kinetic scaling of time implicitly includes a linear scaling of the adsorption rate with both Bi and $\bar{c}_0$. The decrease in adsorption rate for both increasing Bi and increasing $\bar{c}_0$ in Figure 2 amounts to a sublinear increase with both Bi and $\bar{c}_0$ in dimensional variables. The sublinear scaling naturally arises from convection-diffusion limitation in the nonlinear dynamics of the system. Apart from in the initial phase, predictions of the quasi-steady theory practically coincides with the simulations, and thereby also the fits, for $\bar{c}_0 = 1$. Increasing the concentration to $\bar{c}_0 = 20$ leads to significant alteration of the simulation curves. Since there are no knobs to turn for the kinetically scaled quasi-steady theory, regarding changes in concentration $\bar{c}_0$, this leads to equally significant deviations between the simulations and predictions of the quasi-steady theory. The observed dependency of $\bar{c}_0$ is expected, since $\bar{c}_0$ parametrizes time dependency in eq 8, and hence transient behavior in the system dynamics, which is not taken into account in the quasi-steady theory. Physically speaking, the surface simply saturates faster than a steady-state can be achieved in the bulk.

Diffusion Scaling. Figure 3 contains a representative collection of phase plane curves using diffusion scaling, that

Figure 2. Phase plane dynamics using kinetic scaling. Simulation (thick line): numerical solution of eqs 8−10. QST (thin line): quasi-steady theory (eq 25) for corresponding value of Da through eq 30. QST Fit (dashed line): fit of the quasi-steady theory to simulation with Da as free fitting parameter. Parameters: $\bar{c}_0 \in \{1,20\}$, Bi = $\{1,10\}$, Pe = 500.
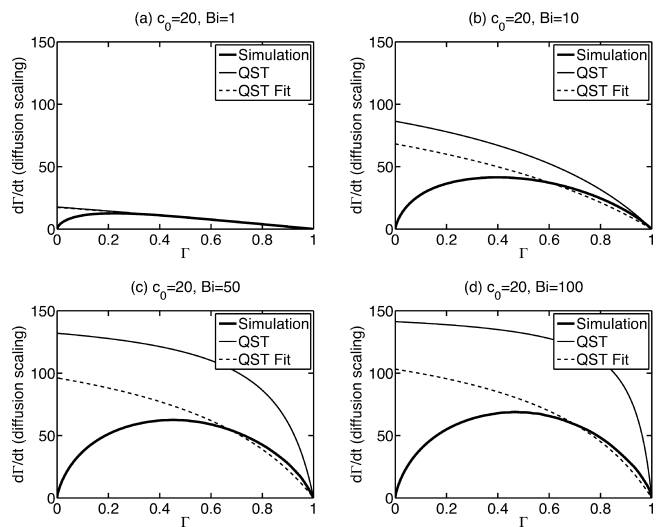
Figure 3. Phase plane dynamics using diffusion scaling. Simulation (thick line): numerical solution of eqs 8−10. QST (thin line): quasi-steady theory (eq 25) for corresponding value of Da through eq 30. QST Fit (dashed line): fit of the quasi-steady theory to simulation with Da as free fitting parameter. Parameters: $\bar{c}_0 = 20$, Bi = $\{1,10,50,100\}$, Pe = 2500.

$\bar{t}^{ks} = k_a c_0 t$. Four different simulations for the combinations of concentrations $\bar{c}_0 \in \{1,20\}$, Bi $\in \{1,10\}$, and Pe = 500 are presented (thick line), each in a separate plot, along with the prediction of the quasi-steady theory for identical parameters (thin line), as well as a fit of the quasi-steady theory to the simulations (dashed line). Importantly, the quasi-steady theory

is, $\bar{t}^{ds} = Dt/h^2$. Four different simulations for the combination of parameters $\bar{c}_0 \in \{20\}$, Bi = $\{1,10,50,100\}$, and Pe = 2500 are presented, each in a separate plot, along with the prediction of the quasi-steady theory for identical parameters, as well as a fit of the quasi-steady theory to the simulations. The universality characteristic obtained with diffusion scaling of time is that the

simulations approach a limiting curve, representing predominantly convection-diffusion limited dynamics, for large Biot numbers. This limiting curve in Figure 3d is observed to have a very symmetric, parabolic-like, characteristic form. Inconsistent with the simulations, quasi-steady theory predicts a linear scaling of adsorption rate with concentration, which is explicit when using diffusion scaling as in Figure 3. This naturally leads to an increasing deviation between quasi-steady theory and simulations for increasing Bi.

Flow Rate Dependency. The nature of the Péclet number dependency is presented in Figure 4, containing four different
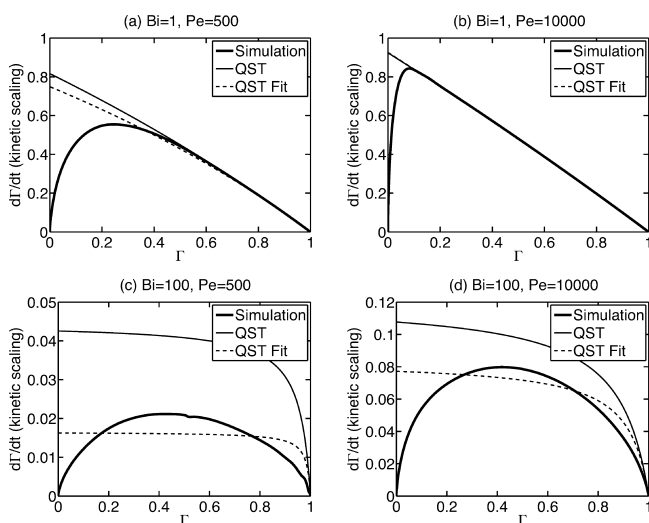
Figure 4. Phase plane dynamics using kinetic scaling. Simulation (thick line): numerical solution of eqs 8−10. QST (thin line): quasi-steady theory (eq 25) for corresponding value of Da through eq 30. QST Fit (dashed line): fit of the quasi-steady theory to simulation with Da as free fitting parameter. Parameters: $\overline{c}_0 = 10$, Bi = {1,100}, Pe = {500,10 000}.

simulations for the combination of parameters $\overline{c}_0 = 10$, Bi = {1,100}, and Pe = {500,10 000}. Again, the simulations are presented, each in a separate plot, along with the prediction of the quasi-steady theory for identical parameters, as well as a fit of the quasi-steady theory to the simulations. Kinetic scaling, that is, $\overline{t}^{ks} = k_a c_0 t$ is applied. Clearly the increase of Péclet number leads to less convection-diffusion limitation. Thereby the simulations approach the diagonal in Figure 4, representing purely adsorption limited linear kinetics, for increasing Pe. This behavior is very clear for Bi = 1, where the dynamics is predominantly kinetically limited. For Bi = 100, where the dynamics is much more convection-diffusion limited, we again observe increased agreement between quasi-steady theory and simulations as the Péclet number is increased. The agreement is however not as good as for Bi = 1. Note that the ordinate axis are different in Figure 4c and d where Bi = 100. The specific case in Figure 4c, where $\overline{c}_0 = 10$, Bi = 100, Pe = 500, is clearly in a regime where the quasi-steady theory has little value, and little ability to fit data well. The approach to adsorption limited dynamics is consistent with a decrease in the Damköhler number as Da ∼ Pe$^{-1/3}$ from eq 30. Figure 4 also serves to show that, due to this slow cubic root dependency, experimental practicalities often precludes to cope with convection-diffusion limitation by simply increasing the flow rate for systems with a high Biot number.

In summary, Figures 2−4 stress some nonlinearities present in the real system dynamics, which are not well captured in the approximate quasi-steady theory.

Error of the Quasi-Steady Theory. The numerical investigation concludes with a quantification of the error of the quasi-steady theory, measured as the relative difference between the Biot number used to fit the quasi-steady theory to simulations, and the Biot number used for the simulation itself. The nondimensional parameter space is spanned by Bi ∈ {1,...,100}, Pe ∈ {500,...,10 000}, for $\overline{c}_0 = \{1,10,20\}$. Figure 5a−
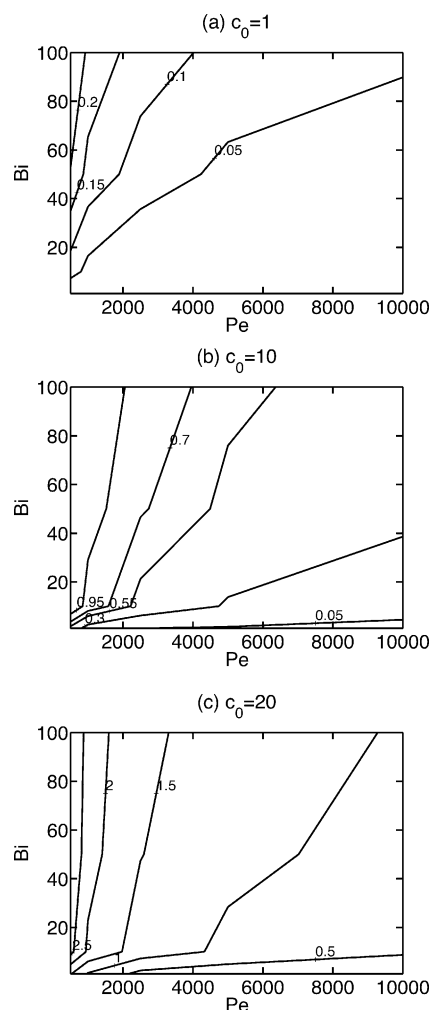
Figure 5. Contour lines of the relative error (Bi^{fit} − Bi)/Bi, in the parameter space (Pe,Bi), for $\overline{c}_0 \in \{1,10,20\}$. The errors increase with increasing Bi, increasing $\overline{c}_0$, and decreasing Pe.

c presents the relative error (Bi^{fit} − Bi)/Bi, by contour lines in the nondimensional parameter space (Pe,Bi) for $\overline{c}_0 = \{1,10,20\}$, respectively. Every contour is labeled with the matching error. Equal for all values of $\overline{c}_0$ is that the error is largest for slow flows of fast binders, that is, small Pe and large Bi numbers. For $\overline{c}_0 = 1$, only relatively minor errors, up to around 0.2 (20%), are observed in the spanned parameter space. However, the quantitative increase of the error with $\overline{c}_0$ is significant. For $\overline{c}_0 = 20$, the errors increase to above 2.5 (250%), which amounts to a factor of 3−4, in the spanned parameter space. Importantly, the quasi-steady theory consequently overestimates the Biot number, and thereby the adsorption rate constant, as long as the error is over a few percent. (Below

errors of a few percent, the fit and the prediction are so close that this is not always the case.) Hence, the parameter planes shown in Figure 5 provide a tool to quantitatively correct experimentally obtained adsorption rate constants, which are derived by fitting data with the quasi-steady theory.

CONCLUSION

This paper presented theoretical and computational investigations of convection, diffusion, and adsorption dynamics in microfluidic surface-based biosensors. The nondimensional Damköhler number Da = $k_a\gamma_m/k_L$, inherent in the quasi-steady theory, was expressed in terms of the Biot number Bi = $k_a\gamma_m h/D$, the Péclet number Pe = $v_m h/D$, and the model geometry. In addition, an analytical solution to the quasi-steady theory was derived. The results provided the regimes of both reliable and unreliable use of the quasi-steady theory for experimental data analysis, by quantifying the error of the quasi-steady theory in the space of parameters for irreversible adsorption. This can be used as a tool to correct adsorption rate constants obtained by fitting the quasi-steady theory to experimental data. We deduced a nondimensional inlet concentration, the value of which measures the critical importance of the inlet concentration in relation to the maximum surface capacity.

AUTHOR INFORMATION

Corresponding Author
*E-mail: rasmush08@gmail.com (R.H.); oh@kt.dtu.dk (O.H.).

Notes
The authors declare no competing financial interest.

REFERENCES

(1) Kim, J. H.-S.; Marafie, A.; Jia, X.-Y.; Zoval, J. V.; Madou, M. J. *Sens. Actuators, B* **2006**, *113*, 281−289.
(2) Mocanu, D.; Kolesnychenko, A.; Aarts, S.; Troost-Dejong, A.; Pierik, A.; Vossenaar, E.; Stapert, H. *J. Biotechnol.* **2009**, *139*, 179−185.
(3) Cheek, B. J.; Steel, A. B.; Torres, M. P.; Yu, Y. Y.; Yang, H. *Anal. Chem.* **2001**, *73*, 5777−5783.
(4) Lu, H.; Koo, L. Y.; Wang, W. M.; Lauffenburger, D. A.; Griffith, L. G.; Jensen, K. F. *Anal. Chem.* **2004**, *76*, 5257−5264.
(5) Roy, B.; Das, T.; Maiti, T. K.; Chakraborty, S. *Anal. Chim. Acta* **2011**, *701*, 6−14.
(6) Yang, K.; Wu, J. *Biomicrofluidics* **2010**, *4*.
(7) Subramaniam, K.; Chakraborty, S. *Microfluid. Nanofluid.* **2011**, *10*, 821−829.
(8) Gervais, T.; Jensen, K. F. *Chem. Eng. Sci.* **2006**, *61*, 1102−1121.
(9) Homola, J. *Chem. Rev.* **2008**, *108*, 462−93.
(10) Homola, J.; Yee, S.; Gauglitz, G. *Sens. Actuators, B* **1999**, *54*, 3−15.
(11) Stenberg, E.; Persson, B.; Roos, H.; Urbaniczky, C. *J. Colloid Interface Sci.* **1991**, *143*, 513−526.
(12) Schuck, P.; Minton, A. *Anal. Biochem.* **1996**, *240*, 262−272.
(13) Myszka, D. G.; He, X.; Dembo, M.; Morton, T. A.; Goldstein, B. *Biophys. J.* **1998**, *75*, 583−594.
(14) Schuck, P. *Biophys. J.* **1996**, *70*, 1230−1249.
(15) Schuck, P.; Minton, A. P. *Anal. Biochem.* **1996**, *240*, 262−272.
(16) Mason, T.; Pineda, A. R.; Wofsy, C.; Goldstein, B. *Math. Biosci.* **1999**, *159*, 123−144.
(17) Noinville, S.; Vidic, J.; Déjardin, P. *Colloids Surf., B* **2010**, *76*, 112−116.
(18) Goldstein, B.; Coombs, D.; He, X.; Pineda, A. R.; Wofsy, C. *J. Mol. Recognit.* **1999**, *12*, 293−299.
(19) Svitel, J.; Boukari, H.; Van Ryk, D.; Willson, R. C.; Schuck, P. *Biophys. J.* **2007**, *92*, 1742−1758.
(20) Rich, R. L.; Myszka, D. G. *J. Mol. Recognit.* **2011**, *24*, 892−914.
(21) Rich, R. L.; Myszka, D. G. *J. Mol. Recognit.* **2010**, *23*, 1−64.
(22) Rich, R. L.; Myszka, D. G. *J. Mol. Recognit.* **2008**, *21*, 355−400.
(23) Rich, R. L.; Myszka, D. G. *J. Mol. Recognit.* **2007**, *20*, 300−366.
(24) Besenicar, M.; Macek, P.; Lakey, J. H.; Anderluh, G. *Chem. Phys. Lipids* **2006**, *141*, 169−178.
(25) Brody, J. P.; Yager, P.; Goldstein, R. E.; Austin, R. H. *Biophys. J.* **1996**, *71*, 3430−3441.
(26) Bird, R. B.; Stewart, W. E.; Lightfoot, E. N. *Transport phenomena*, 2nd ed.; J. Wiley: New York, 2002.
(27) Alvarez, N. J.; Walker, L. M.; Anna, S. L. *Phys. Rev. E* **2010**, *82*, 011604.
(28) Squires, T. M.; Messinger, R. J.; Manalis, S. R. *Nat. Biotechnol.* **2008**, *26*, 417−426.
(29) Goren, M.; Galley, N.; Lennox, R. B. *Langmuir* **2006**, *22*, 1048−1054.
(30) (a) Sonesson, A. W.; Callisen, T. H.; Brismar, H.; Elofsson, U. M. *Colloids Surf., B* **2008**, *61*, 208−215. (b) Sonesson, A. W.; Elofsson, U. M.; Callisen, T. H.; Brismar, H. *Langmuir* **2007**, *23*, 8352−8356.